Feature Article

Electrochemical Oxidation of 8-Oxo-2′-Deoxyguanosine on Glassy Carbon, Gold, Platinum and Tin(IV) Oxide Electrodes

Jan Langmaier,*[a] *Zdeněk Samec*,[a] *Eva Samcová*[b]

[a] J. Heyrovský Institute of Physical Chemistry, Academy of Sciences of the Czech Republic, Dolejškova 3, 182 23 Prague 8, Czech Republic
*e-mail: jan.langmaier@jh-inst.cas.cz
[b] Charles University, 3rd Faculty of Medicine, Centre for Biomedical Sciences, Ruská 87, 100 00 Prague 10, Czech Republic

Abstract
Cyclic voltammetry was used to investigate the oxidation of 8-oxo-2′-deoxyguanosine (8-oxo-dG) on the glassy carbon (GC), platinum, gold and SnO_2 electrodes over a range of the sweep rate, 8-oxo-dG concentration and the solution pH. Reaction mechanism that is common to all these electrodes involves the two-electron two-proton charge transfer step followed by the irreversible chemical reaction(s). Rate of the charge transfer reaction decreases with the increasing solution pH (GC, Pt, Au), and depends on the nature of the electrode material following the sequence $GC > Pt, Au \gg SnO_2$. These effects can be related to the degree of oxidation of the electrode surface (Pt, Au, SnO_2), or to the density of the active surface sites (GC). Any of these electrodes can be used for the fabrication of an amperometric detector for 8-oxo-dG .

Keywords: Electrochemical oxidation, 8-Oxo-2′-deoxyguanosine, Voltammetry, Electrode material

1. Introduction

The occurrence of 8-oxo-2′-deoxyguanosine (8-oxo-dG, Scheme 1) in biological fluids, especially in human urine, has been proposed to be a consequence of the in vivo oxidative DNA damage [1,2]. Several methods for the determination of 8-oxo-dG in urine have been developed including gas chromatography-mass spectroscopy (GC-MS) [3], high performance liquid chromatography (HPLC) [4–6] and high performance capillary electrophoresis (HPCE) [7]. Most common method utilizes the solid phase extraction and HPLC with amperometric detection [4–6], which is based on the electrochemical oxidation of 8-oxo-dG on a glassy carbon (GC) electrode. Amperometric detection has been shown to be 3 orders of magnitude more sensitive than

UV absorbance [4, 5]. Differential pulse voltammetry can be used for direct determinations of the parent base, 8-oxo-guanine [8].

Mechanism and products of the electrochemical oxidation of 8-oxo-dG on GC and pyrolytic graphite (PG) electrodes have been analyzed under various reaction conditions [8–10]. The results point to an overall two-electron oxidation process accompanied by the dissociation of two protons, which is followed by the cascade of the chemical pathways yielding a variety of products [9, 10], cf. Scheme 1. The oxidation intermediates and products are difficult to detect by cyclic voltammetry, except for those adsorbing strongly on the electrode surface [8–10]. Apart from minor differences in the voltammetric responses of the PG and GC electrodes [10], there has been no evidence that
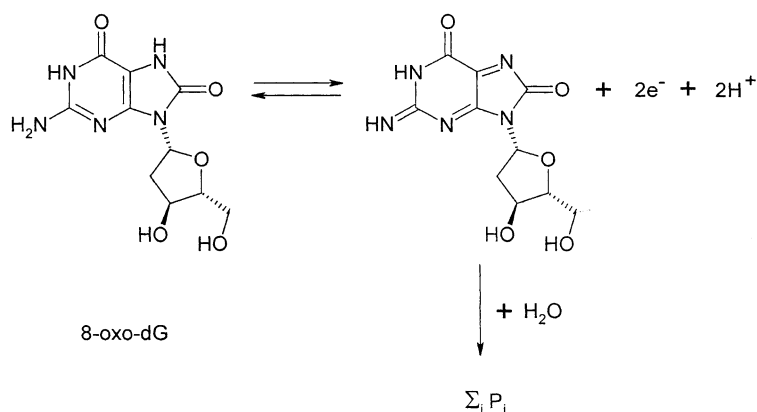
Scheme. 1.

the electrode material plays a significant role in the oxidation of 8-oxo-dG. Nevertheless, the involvement of the electrode surface can be an important factor influencing the reproducibility of the electrochemical detection of 8-oxo-dG.

The aim of this work was to examine the effect of the electrode material more thoroughly. A series of voltammetric measurements of the 8-oxo-dG oxidation has been carried out on the GC, platinum, gold and SnO₂ electrodes over a range of the sweep rate, 8-oxo-dG concentration and the solution pH. We shall show that the 8-oxo-dG oxidation follows the same mechanism on all these electrodes, though the rate of the electrode reaction at a constant potential can be considerably different. The origin of the effect of the electrode material will be discussed, as well as the possibility of using these electrodes for the fabrication of an amperometric detector of 8-oxo-dG.

2. Experimental

Analytical reagent grade chemicals (Sigma, Merck), and highly purified and deionized water (GORO System, Czech Republic) were used for the preparation of solutions of 8-oxo-2′-deoxyguanosine in 0.1 M HClO₄ (pH 1.1), McIlvaine buffer (pH 2–7) or Sörensen buffer (pH 7.2). Tested solutions were deoxygenated before measurements by argon bubbling.

Voltammetric measurements were carried out at the ambient temperature in an all-glass cell by using the three-electrode potentiostat (Model 273A, EG&G PAR), which was equipped with the operating software (M270, EG&G PAR). Pt (10 μm diam., BAS, USA), Au (10 μm diam., BAS, USA) and GC (11 μm diam., BAS, USA) microelectrodes

were polished mechanically by a 3 μm and 0.25 μm diamond paste (Winter Diaplast, Germany), and electrochemically by cyclic polarization in 0.1 M HClO₄ between the positive and negative potential limits (1 mA cm⁻²). Similar pretreatment was employed for the homemade Pt (0.5 mm diam., home), Au (1.0 mm diam.) and GC (2.5 mm diam.) conventional electrodes, while SnO₂ (F) coated-glass electrode (0.14 cm², Nippon Sheet Glass, 10 Ω/□) was polished only electrochemically. A Pt wire and the Ag | AgCl | sat. KCl electrode were used as the counter and the reference electrode, respectively. All measurements were carried out at ambient temperature ($22 \pm 2\,^{\circ}$C).

3. Results and Discussion

Figure 1 shows the voltammetric behavior of the Pt, GC and Au microelectrodes in the absence and the presence of 8-oxo-dG in the solution. In the experimental range of the sweep rates (5–100 mV s⁻¹) all three microelectrodes operate in the steady state regime and the voltammetric curve of the 8-oxo-dG oxidation has the shape of a wave. It can be seen that the presence of 8-oxo-dG and/or its oxidation products has rather small effect on the surface charge transfer reactions, cf. a minor blocking of the surface oxide formation on Au and Pt. However, a long term scanning (ca. 2 h) in the potential range of the 8-oxo-dG oxidation leads to a passivation of the electrode surface accompanied by a decrease in the measured current. The electrode activity had to be restored by cyclic polarization in 0.1 M HClO₄ in the absence of 8-oxo-dG.

The anodic half-wave potential $E_{1/2}$ depends on the solution pH, cf. Figure 2 and the slopes $dE_{1/2}/d$ pH given in Table 1. The slope of -52 mV/pH obtained for the GC
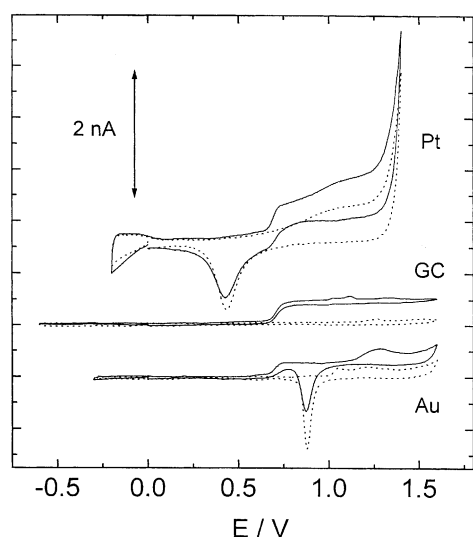

Fig. 1. Cyclic voltammograms of the Pt, GC and Au microelectrodes in the absence (dotted line) and the presence (full line) of 0.2 mM 8-oxo-dG, pH 1.1. Sweep rate 20 mV s⁻¹.
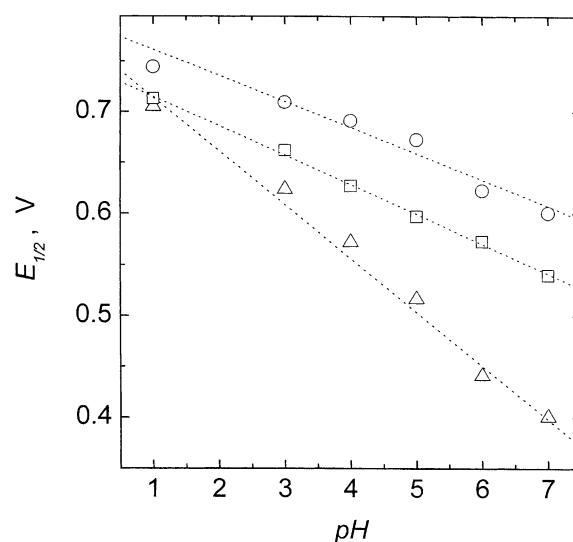

Fig. 2. Plot of the half-wave potential $E_{1/2}$ vs. pH for 0.2 mM 8-oxo-dG and the Pt (○), Au (□) and GC (△) microelectrode. Sweep rate 20 mV s⁻¹.

Table 1. Voltammetric parameters of the 8-oxo-dG oxidation on various electrodes at pH 1.1 and pH 7.2 (in parentheses).

Electrode	$dE_{1/2}/d$ pH (mV)	$10^{-3} \, d(i_p{}^a c_0{}^{-1})/dv^{1/2}$ (A cm mol^{-1} V$^{-1/2}$)	$dE_p{}^a/d \log v$ (mV)	$E_p{}^a - E_{p/2}{}^a$ (mV)
GC	-52	1.3 (1.1)	27 (33)	38 (62)
Au	-29	1.5 (1.2)	16 (31)	26 (114)
Pt	-23	1.2 (1.7)	17 (55)	27 (144)
SnO$_2$	-5 [a]	0.6 (0.6)	59 (120)	125 (192)

[a] $dE_p{}^a/d$ pH
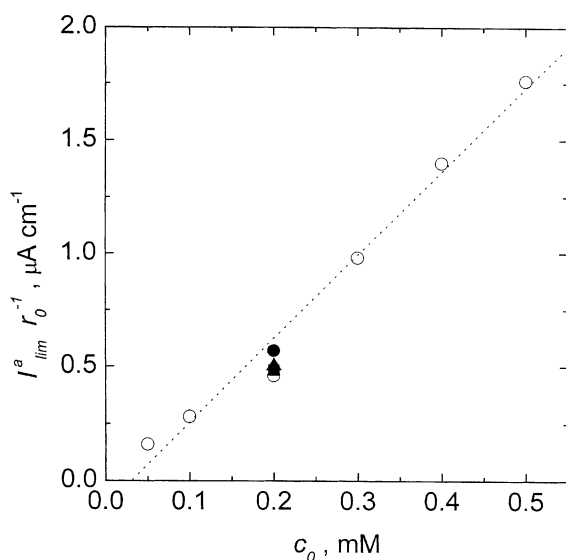
Fig. 3. Plot of $I_{lim}{}^a r_0{}^{-1}$ vs. the concentration c_0 of 8-oxo-dG for the Pt microelectrode, pH 5 (○); and the Pt (●), GC (■) or Au (▲) microelectrodes, pH 1.1, sweep rate 20 mV s^{-1}.

electrode is comparable with the slope of -59 mV/pH or -74 mV/pH reported for the GC [8] or PG [9] electrode, respectively.

The limiting anodic current $I_{lim}{}^a$ is proportional to the bulk concentration c_0 of 8-oxo-dG (0.05 – 0.5 mM), while the effect of the solution pH and the nature of the electrode material is rather negligible, cf. Figure 3. Seven independent measurements of the limiting current for 0.2 mM 8-oxo-dG (pH 1) for each electrode provided the values of 0.25 ± 0.02 nA (Au), 0.29 ± 0.03 nA (Pt) and 0.27 ± 0.04 nA (GC) after a correction for the background current.

Coulometric analysis based on the electrolysis of 8-oxo-dG on a large-area (ca. 5 cm^2) gold electrode in the potential range of the limiting current yielded the number of electrons consumed in the overall reaction $n = 2.0 \pm 0.1$. This value agrees well with the literature data for the GC and PG electrode [9].

Figure 4 shows the voltammetric behavior of the conventional GC, Au and SnO$_2$ electrodes. In this case, the electrode process is apparently controlled by linear diffusion, and the voltammetric curve of the 8-oxo-dG oxidation has the shape of a peak. The background correction of the voltammograms measured with the SnO$_2$ electrode was rather negligible, cf. the inset in Figure 4A. The behavior of
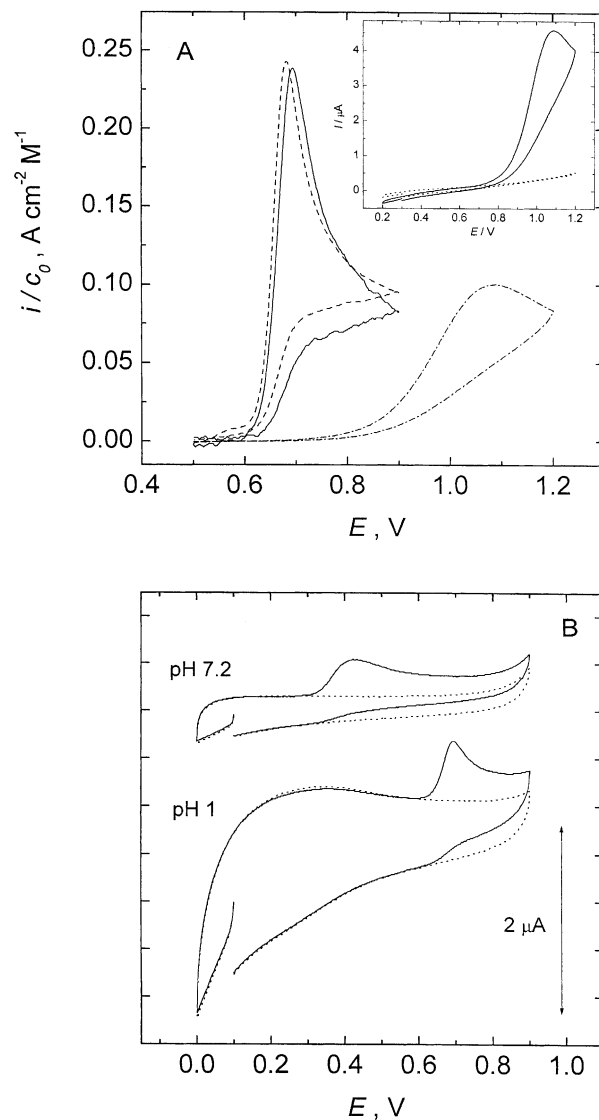

Fig. 4. A) Background corrected voltammograms of the 8-oxo-dG oxidation normalized to the electrode area A and to the bulk concentration c_0 for the conventional GC (full), Au (dashed) and SnO$_2$ (dashed-and-dotted) electrodes at pH 1, at the sweep rate 20 mV s^{-1}. Inset: voltammogram for the SnO$_2$ electrode in the absence (dotted) and the presence (full) of 0.3 mM 8-oxo-dG. B) Cyclic voltammograms of the conventional GC electrode at pH 1.1 and pH 7.2 in the presence (full line) and the absence (dotted line) of 5×10^{-5} M 8-oxo-dG.
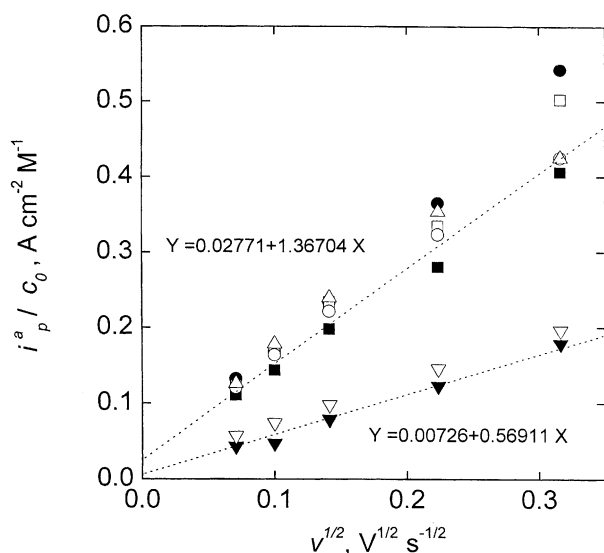
Fig. 5. Plot of $i_p^a c_0^{-1}$ vs. $v^{1/2}$ for the oxidation of 8-oxo-dG at pH 1 (empty points) and pH 7.2 (solid points) on the conventional Pt ($\circ$,$\bullet$), GC($\triangle$), Au ($\square$,$\blacksquare$) and SnO$_2$ ($\triangledown$,$\blacktriangledown$) electrodes.

Fig. 6. Plot of E_p^a vs. log$v$ for the oxidation of 8-oxo-dG, pH 1, on the conventional Pt ($\circ$), GC($\triangle$), Au ($\square$) and SnO$_2$ ($\triangledown$) electrodes.

the GC electrode indicated that the background and the 8-oxo-dG oxidation currents are additive, cf. Figure 4B. On the other hand, the correction was less satisfactory for the Pt and Au electrodes, in particular at a higher pH, cf. also the voltammetric behavior of the microelectrodes shown in Figure 1. The parameters inferred from the background corrected voltammograms are summarized in Table 1.

The anodic peak current I_p^a (or the peak current density i_p^a) is proportional to the concentration of 8-oxo-dG (0.5 – 5.0 mM), and to the square root of the sweep rate v (5 – 100 mV s^{-1}), cf. Figure 5. The slopes d($i_p^a c_0^{-1}$)/d$v^{1/2}$ for the GC, Au or Pt electrodes are comparable, but approximately twice as large as that for the SnO$_2$ electrode.

With the increasing sweep rate, the anodic peak shifts towards more positive potentials, cf. Figure 6. Again, the slopes dE_p^a/d log$v$ for the GC, Au or Pt electrodes are comparable, but considerably lower than that for the SnO$_2$ electrode.

In agreement with the results obtained for the micro-electrodes, the change in the solution pH has no apparent effect on the anodic peak current or the slope d($i_p^a c_0^{-1}$)/d$v^{1/2}$, while it has an effect on the anodic peak potential, dE_p^a/d pH $\approx$ d$E_{1/2}$/d pH . With the increasing pH, the slope dE_p^a/d log$v$ increases and a significant peak broadening is observed, which can be characterized by the increasing value of the difference between the peak and half-peak potential, $E_p^a - E_{p/2}^a$, cf. Table 1.

Apart from somewhat different values of the voltammetric parameters given in Table 1, the oxidation of 8-oxo-dG on the GC, Au, Pt and SnO$_2$ electrodes has a number of common features, which points to the same reaction mechanism. In accordance with the accepted reaction Scheme 1 [9, 10], this mechanism can be described as the two-electron two-proton charge transfer (E) followed by the
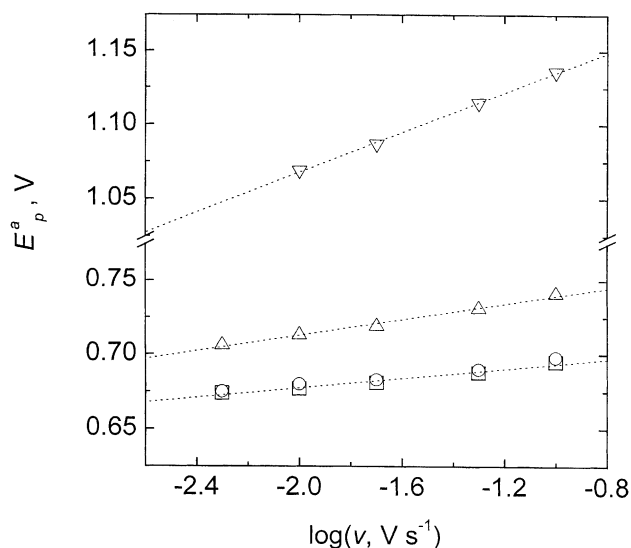
irreversible chemical reaction(s) yielding a variety of products (C), an EC mechanism

$$8\text{-oxo-dG} \leftrightarrow P + 2\,e^- + 2\,H^+ \tag{1}$$

$$P \rightarrow \sum_i P_i \tag{2}$$

where P is the unstable diimine intermediate and P$_i$ are the final products of the oxidation reaction [10], cf. also Scheme 1. Charge transfer reaction, Equation 1, is probably a sequence of one-electron and one-proton steps, which, however, are difficult to detect experimentally [9, 10].

Square-wave voltammetric measurements provided convincing evidence that the charge transfer reaction on a GC electrode is reversible (E_r) [8], i.e., the net irreversibility of the process is due to the following irreversible chemical reaction (C$_i$), Equation 2. In buffered solutions, the effects of the proton transport can be neglected and the boundary condition for the transport controlled by the linear diffusion can be written as

$$E = E^{0'} + \frac{RT}{2F} \ln \frac{c_P(0,t)a_{H^+}^2}{c_{8-oxo-dG}(0,t)} \tag{3}$$

where $E^{0'}$ is the formal potential of the charge transfer reaction, $c_i(0,t)$ are the concentrations of P or 8-oxo-dG at the electrode at time t, and a_H is the proton activity. Obviously, the half-wave potential $E_{1/2}$ or the anodic peak potential E_p^a should shift with the solution pH with a slope of dE_p^a/d pH = d$E_{1/2}$/d pH = $-$ 59 mV, which indeed is observed [8], cf. also Table 1. The other diagnostic criteria are

based on the values of the voltammetric parameters $dE_p^a/d\log v = 30/n = 15$ mV, $E_p^a - E_{p/2}^a = 57/n = 28$ mV and $d(i_p^a c_0^{-1})/dv^{1/2} = 2.99 \times 10^5 \, n^{3/2} \, D^{1/2}$ A cm mol^{-1}V$^{-1/2}$ that are predicted for an E_rC_i mechanism [11]. The diffusion coefficient D of 8-oxo-dG can be evaluated from independent measurements of the steady state anodic limiting current I_{lim}^a on the GC, Pt and Au microelectrodes. For a microdisc of the radius r_0, this limiting current should be given by [12],

$$I_{lim}^a = 4FDr_0c_0 \tag{4}$$

The values of I_{lim}^a for 0.2 mM 8-oxo-dG (pH 1) listed above correspond to the diffusion coefficient $D = (3.3 \pm 0.3) \times 10^{-6}$ cm^2 s^{-1} (Au), $(3.7 \pm 0.3) \times 10^{-6}$ cm^2 s^{-1} (Pt) and $(3.4 \pm 0.4) \times 10^{-6}$ cm^2 s^{-1} (GC). On this basis, the expected value of $d(i_p^a c_0^{-1})/dv^{1/2} = 1.6 \times 10^3$ A cm mol^{-1}V$^{-1/2}$. At pH 1, the experimental parameters for the GC electrode are close to that expected, cf. Table 1. When the solution pH is increased, the peak broadening, i.e., an increase in the value of $E_p^a - E_{p/2}^a$ and in the slope $dE_p^a/d\log v$ is observed which point to a decrease in the rate constant of the charge transfer reaction, Equation 1. It is noteworthy, that these changes apparently accompany a considerable decrease in the background current, cf. Figure 4B, which can be considered to be a measure of the density of the surface active sites or the surface roughening of a GC electrode [13].

The shape of the voltammogram, the voltammetric parameters and the absence of the pH effect on the anodic peak potential (Table 1) indicate that the charge transfer reaction on the SnO$_2$ electrode is irreversible. This irreversibility apparently originates from the very slow charge transfer reaction on the oxidized metal surface. For an E_iC_i mechanism, the voltammetric parameters should depend on the number of electrons transferred up to, and including the rate determining step, n_{app}, and on the anodic charge transfer coefficient α_a: $dE_p^a/d\log v = 30/n_{app}\alpha_a$ mV, $E_p^a - E_{p/2}^a = 57/n_{app}\alpha_a$ mV and $d(i_p^a c_0^{-1})/dv^{1/2} = 2.99 \times 10^5 \, n \, (n_{app}\alpha_a)^{1/2} \, D^{1/2}$ A cm mol^{-1}V$^{-1/2}$ [11]. The experimental slope $dE_p^a/d\log v$, as well as the difference $E_p^a - E_{p/2}^a$, corresponds to $n_{app}\alpha_a \approx 0.25 - 0.5$ depending on the solution pH. The experimental value of the parameter $d(i_p^a c_0^{-1})/dv^{1/2}$, cf. Table 1, agrees well with the value of $(0.6-0.8) \times 10^3$ A cm mol^{-1}V$^{-1/2}$ calculated for $n = 2$, $D = 3.3 \times 10^{-6}$ cm^2 s^{-1}, and $n_{app}\alpha_a \approx 0.25 - 0.5$. It can be concluded that the oxidation of 8-oxo-dG on the SnO$_2$ electrode is also a two-electron process.

The Au and Pt electrodes exhibit the intermediate voltammetric behavior. At pH 1, the voltammetric parameters reach the values predicted for an E_rC_i mechanism. When the solution pH is increased, an increase in the experimental slope $dE_p^a/d\log v$ and in the difference $E_p^a - E_{p/2}^a$ is observed as for the GC electrode, but the effect is much more pronounced. A very slow kinetics of the 8-oxo-dG oxidation on the SnO$_2$ electrode indicates that the formation of the surface oxides on the Au and Pt should also have an inhibitory effect on the charge transfer step, Equation 1. The rate of the charge transfer apparently decreases with the increasing solution pH, in an agreement with the observation that the onset of the surface oxide

formation on Pt and Au shifts negative [14]. The lower values of the slope $dE_{1/2}/d$ pH $= -29$ and -23 mV for the Au and Pt electrode, respectively, can then be a consequence of two opposite tendencies. One tendency is a shift in the equilibrium in the Reaction 1 to the right hand side and the corresponding negative shift in the anodic peak potential. The other one is the decreased value of the charge transfer rate constant leading to the peak broadening and to a positive shift in the peak potential.

Amperometric detection of 8-oxo-dG in HPLC or HPCE is based on measurements of the limiting diffusion current of the 8-oxo-dG oxidation under the steady state hydrodynamic flow conditions. Cyclic voltammetry of the GC, Pt and Au microelectrodes shows that there should be no difference between these electrodes as to the sensitivity of detection. In a preliminary study [15], we have tested the amperometric detector with the tubular Pt electrode [16] with promising results, e.g., 8-oxo-dG was determined with the detection limit of 9.8 nmol/L. Since the voltammetric results for the SnO$_2$ electrode also point to a two-electron oxidation process, we expect that the same steady state diffusion current and the sensitivity can be achieved as with the GC, Pt and Au electrode, provided the electrode potential is chosen sufficiently positive. An advantage of the amperometric detection using the SnO$_2$ electrode could be the very low background current, cf. the inset in Figure 4A. Since the thin films of SnO$_2$ deposited on a glass or quartz substrate are optically transparent, there exists the viable possibility of developing a spectroelectrochemical detector on this basis.

4. Conclusions

Mechanism of electrochemical oxidation of 8-oxo-2′-deoxyguanosine on the GC, Pt, Au and SnO$_2$ electrode can be classified as an EC type involving the two-electron two-proton charge transfer step followed by the irreversible chemical reaction(s). The rate of the charge transfer reaction decreases with the increasing solution pH, and depends on the nature of the electrode material following the sequence GC > Pt, Au >> SnO$_2$. These effects can be related to the degree of oxidation of the electrode surface (Pt, Au, SnO$_2$), or to the density of the active surface sites (GC). Under the steady state diffusion conditions, the sensitivity of the electrochemical detection of 8-oxo-dG using either GC, Pt, Au or SnO$_2$ electrode should be comparable.

5. Acknowledgement

6. References

[1] K. C. Cundy, R. Kohen, B. N. Ames, *Basic Life Sci.* **1988**, *49*, 479.

[2] M. K. Shigenaga, C. J. Gimeno, B. N. Ames, *Proc. Natl. Acad. Sci. USA* **1989**, *86*, 9697.

[3] A. J. Teixeira, J. H. Gommers, G. van der Werken, J. G. Westra, J. F. C. Stavenuiter, A. P. J. M. de Jong, *Anal. Biochem.* **1993**, *214*, 474.

[4] R. A. Floyd, J. J. Watson, J. Harris, M. West, P. K. Wong, *Biochim. Biophys. Res. Comm.* **1986**, *137*, 841.

[5] R. A. Floyd, J. J. Watson, P. K. Wong, D. H. Altmiller, R. C. Rickard, *Free Radic. Res. Comm.* **1986**, *1*, 163.

[6] C. Tagesson, M. Källberg, C. Klintenberg, H. Starkhammar, *Eur. J. Cancer* **1995**, *31A*, 934.

[7] D. J. Weiss, C. E. Lunte, *Electrophoresis* **2000**, *21*, 2080.

[8] A. M. Oliveira Brett, J. A. P. Piedale, S. H. P. Serrano, *Electroanalysis* **2000**, *12*, 969.

[9] R. N. Goyal, G. Dryhurst, *J. Electroanal. Chem.* **1982**, *135*, 75.

[10] R. N. Goyal, N. Jain, D. K. Garg, *Bioelectrochem. Bioenerg.* **1997**, *43*, 105.

[11] R. S. Nicholson, I. Shain, *Anal. Chem.* **1964**, *36*, 706.

[12] A. J. Bard, L. R. Faulkner, *Electrochemical Methods: Fundamentals and Applications*, 2nd Ed., Wiley, New York, **2001**, p. 171.

[13] R. L. McCreery in *Electroanalytical Chemistry*, Vol. 17 (Ed: A. J. Bard), Marcell Dekker, New York **1991**, pp. 221–374.

[14] B. E. Conway, *Prog. Surf. Sci.* **1995**, *49*, 331.

[15] E. Samcová, P. Marhol, F. Opekar, J. Langmaier, V. Kvasnicová, *Proc. 25th Int. Symp. Capillary Chromatography*, May 13–17, **2002**, Riva del Garda, Italy.

[16] J. Cvacka, F. Opekar, J. Barek, J. Zíma, *Electroanalysis* **2000**, *12*, 39.